Mechanical behaviour of FRP composite materials at elevated temperature

Inês Cruz Mina Rosa Instituto Superior Técnico

Abstract

The growing use of fibre-reinforced polymer (FRP) materials in civil engineering can be explained by the several advantages they present over traditional materials, namely their lightness, high strength and durability. However, the knowledge about the behaviour of these materials is still underdeveloped, in particular when subjected to elevated temperatures or fire. In fact, the properties of FRP materials experience a significant reduction at moderately elevated temperatures, especially when approaching the glass transition temperature (T_g), which generally varies between 80 ºC and 150 ºC. In the present paper, experimental and analytical studies about the behaviour of glass fibre reinforced polymer (GFRP) pultruded profiles at elevated temperatures are presented. The main objective was to characterize the mechanical behaviour of this material up to temperatures near the T_g. The experimental campaign consisted of shear and compressive tests, performed in specimens cut from pultruded GFRP profiles, with rectangular and I cross-sections, respectively, exposed from ambient temperature up to 180 ºC. In each experimental series, the mechanical response of the material as a function of temperature was assessed, namely in terms of load-displacement curves, stiffness, stress-strain curves, strength, longitudinal elasticity modulus in compression, shear modulus and failure modes. The results obtained confirmed that the mechanical properties of GFRP profiles present a considerable reduction with elevated temperature: at 180 ºC the shear and compressive strengths were reduced to 88% and 42%, respectively, compared to the values at ambient temperature. Regarding the analytical study, the empirical formulations used in the present study provided reliable estimates for the degradation with temperature of the compressive and shear strengths and for the shear modulus.

Keywords: GFRP pultruded profiles, elevated temperature, mechanical properties, shear, compression, degradation models.

1. Introduction

Fibre-reinforced polymer (FRP) materials have been increasingly used in civil engineering applications since the 1960s, due to the advantages they present compared with traditional materials, namely low weight, good insulation properties, high strength and durability, even in aggressive environments. Nevertheless, the widespread use of FRPs as structural materials has been conditioned by their susceptibility to instability phenomena, absence of specific regulation and, especially, their vulnerability to fire and high temperatures, which is accompanied by smoke, soot and toxic volatiles release when the organic matrix decomposes (at temperatures of about 300-500 ºC) **[1]**.

Although some studies available in the literature have shown that the mechanical properties of FRPs are severely deteriorated at moderately elevated temperatures, especially when approaching the glass transition temperature of the polymeric matrix **[1]** (generally in the range of 60-140 ºC **[2]**), this issue is still not well understood and further studies are needed. In the attempt to respond to the above mentioned concerns, some studies were already conducted, mainly focusing on the tensile behaviour, which remains better characterized than the shear and compressive ones. Moreover, it is worth mentioning that the mechanical behaviour of these materials has only been tested up to around 250-300 ºC. In this regard, experimental data is still scarce, mainly because, on one hand, these tests involve temperature ranges which are not easily attained in most thermal chambers; and, on the other hand, the test setups generally involve problems regarding slippage of the specimens in the grips of the testing machines or premature failures on the extremities of the tested specimens **[3]**.

Regarding the shear behaviour at elevated temperatures, Bai & Keller **[4]** and Correia *et al.* **[2]** performed tests on GFRP materials in which the tested specimens were subjected to a 10º off-axis tensile load (angle with the pultrusion direction), thus simulating a shear stress. Bai & Keller **[4]** studied the strength degradation with temperature of glass-polyester pultruded laminates (350×30×10 mm), exposed to temperatures ranging from 20 ºC to 220 ºC. The results obtained showed shear strength retention of 13% at 220 ºC (compared to the strength at ambient temperature).

Correia *et al.* **[2]** tested rectangular specimens (800 mm long with a 20×10 mm cross-section, cut from a flat pultruded GFRP profile) heated up to temperatures from 20 ºC to 250 ºC (T_g between 96-152 ºC). As expected, the specimen's shear strength presented a significant reduction with temperature, especially pronounced at the temperature range that includes the glass transition process (in this case, between 90 and 150 ºC); at 250 ºC, the residual shear strength was only 11% of the corresponding value at ambient temperature. Regardless of the tested temperature, the specimens exhibited a linear behaviour up to failure, which was due to the test setup adopted in this study, with a considerable contribute of the axial fibres. This behaviour was also observed by Bai & Keller **[4]** (who adopted a similar test setup). Lastly, the failure modes observed in both studies were characterized by the rupture of both the matrix and the superficial mats, with the longitudinal fibres remaining intact, and the failure surfaces being orientated roughly at 10º with the pultrusion direction.

Correia *et al.* **[2]** also attempted to evaluate the effect of elevated temperatures on the shear modulus of the above mentioned GFRP pultruded profiles. However, the strain measuring technique used in that study (strain gauge rosettes) only provided reliable results for temperatures up to 120 ºC.

Moreover, the test setup adopted (applying a 10º off-axis tensile load, as in the experiments by Bai & Keller) did not simulate correctly a pure shear stress state, therefore the results obtained could not provide accurate estimates of the shear modulus variation with temperature.

In what concerns compressive strength, Correia *et al.* **[2]** studied the mechanical behaviour of GFRP pultruded profiles (T_g between 96-152 ºC) with an I cross-section (dimensions of 120×60 mm, 6 mm thick walls). The authors tested 50 mm high (short) columns under compression (up to failure) from temperatures ranging from ambient temperature to 250 ºC. Despite an initial non-linear response (due to minor adjustments between the specimens and the loading plates), the tested columns exhibited an approximate linear behaviour up to failure. As expected, the compressive strength presented a considerable reduction with temperature, higher than that obtained for the compressive stiffness. At 250 ºC, the residual compressive strength was only 5% of the strength at ambient temperature. Even for a temperature as low as 60 ºC, which according to Correia *et al.* can be easily reached in exterior applications or roof structures, the strength degradation was already 30%. The columns tested exhibited two different failure modes: (i) at ambient temperature, failure occurred by crushing and wrinkling of the material, together with ply delamination; (ii) at elevated temperature, failure tended to concentrate at mid-height of the column, being triggered by resin softening during the glass transition process, which consequently led to detachment and buckling (kinking) of the glass fibres.

Prior to the above mentioned study, Bai & Keller **[4]** tested tubular GFRP columns (40 mm of diameter, 3 mm of wall thickness and 300 mm of height) exposed to temperatures ranging from ambient temperature (20 ºC) to 220 ºC. Wang *et al.* **[5]** studied GFRP C-channel columns (T_g=120 ºC; cross-section dimensions of 100×30×4 mm and 30 mm height) heated up from ambient temperature (20 ºC) to 250 ºC. Although in all three experimental campaigns mentioned above different specimens' geometries were used, the strength degradation with temperature and the failure modes were similar, as Correia *et al.* reports in **[6]**. In the case of Wang *et al.* and Bai & Keller, the residual values of the compressive strength were 10% and 8%, respectively, at 220 ºC and 250 ºC, being slightly higher than the values obtained by Correia *et al.* **[2]** (5% at 250 ºC).

Apart from the above mentioned experimental studies, there are no data available in the literature regarding the influence of temperature on the mechanical properties of GFRP pultruded profiles. Furthermore, there are still no studies in the literature exploring the effects of elevated temperature on relevant mechanical properties, such as the elasticity modulus (either in tension or in compression) or the shear modulus. Moreover, there is still a need to validate existing degradation models, or to develop new ones, capable of accurately predicting the reduction of those properties with temperature. For all the reasons mentioned above, further studies on the mechanical behaviour of FRP materials when exposed to elevated temperatures are not only relevant but needed.

In this context, this paper presents the results of an experimental campaign, developed within the author's master dissertation, about the mechanical behaviour of GFRP pultruded profiles when exposed to elevated temperatures. To further understand the influence of temperature on the mechanical performance of these materials, specimens were tested under shear and compression and then the results obtained were subsequently analysed in terms of strength, stiffness and failure modes, as well as shear modulus (shear tests) and longitudinal elasticity modulus in compression (compressive tests). The tested temperatures ranged from ambient temperature up to 180 ºC, thus including the glass transition temperature (set between 100 to 152 ºC, determined in **[7])**, which is known to have a significant contribution to the FRP's mechanical properties degradation **[6]**.

The final part of this paper assesses the accuracy of five different models (four of them empirical and one semi-empirical) suggested in the literature to simulate/predict the results obtained experimentally. Although Correia *et al.* **[2]** have already shown that these models can be successfully used to describe tensile, compressive and shear strength reductions with temperature, their ability to describe different mechanical properties, namely the shear modulus and the elasticity modulus (in tension and compression) is yet to be demonstrated. The five models referred above (and described in detail in section **4**) were applied herein not only to the strength results (those obtained in the present study and those available in the literature), but also to the shear modulus data obtained in the present study.

2. Description of the experimental programme

2.1. Materials

The materials used in the experimental campaign were supplied by *Fiberline DK* and consisted of GFRP pultruded profiles with the two following cross-sections: a flat plate (850×150 mm, 10 mm thick), used in the shear tests, and an I-section profile (120×60 mm, 8 mm thick), which was used in the compressive tests. The inorganic content in mass of those cross-sections, determined from burn-off-tests, was 70% **[8]** and 69% **[9]** respectively. Both sections are made of alternating layers of unidirectional continuous E-glass fibre rovings and strand mats of randomly oriented continuous fibres. The glass fibres were embedded in a polyester resin matrix, whose reference glass transition temperature T_g was determined by a DMA analysis performed by Morgado *et al.* **[7]**. The values of T_g determined were 100 ºC, 136 ºC and 152 ºC, obtained based on the extrapolated onset of the sigmoidal change in the storage modulus curve, the peak of the loss modulus curve and the peak of loss factor curve, respectively. It is worth mentioning that the materials used in the present experimental campaign were similar to those tested by Correia *et al.* **[2]** in shear and compression (previously described in section **1**).

2.2. Shear tests at elevated temperature

Shear tests were performed according to the test method suggested in ASTM 5379/D 5379M – 05 **[10]**, designated as *V-Notched Beam Test*, and using the test setup illustrated in **Fig. 2**.

The coupons (**Fig. 1**) consisted of rectangular flat strips (75×20 mm, 10 mm thick), cut from the flat profile, with their length aligned with the pultrusion direction, and two symmetrical centrally located V-notches. The coupons were placed in a special metallic fixture (**Fig. 3 a**), which was loaded in compression, using a universal testing machine (**Fig. 2**); this setup allowed subjecting the coupons to a shear stress state, monitored at their central part.

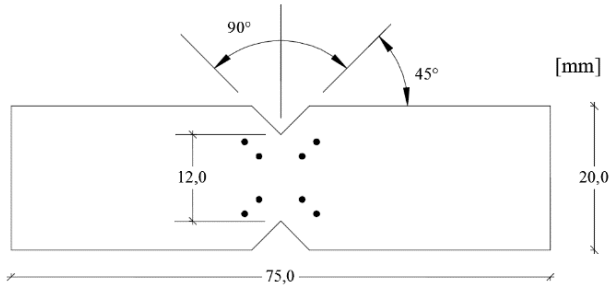

Fig. 1: Shear coupons – dimensions and target scheme.

The experimental procedure consisted of two stages: in the first stage, the coupons were heated up to a predefined temperature ranging from ambient temperature to 180 ºC (16 ºC, 60 ºC, 100 ºC, 140 ºC and 180 ºC), using a *Tinius Olsen* thermal chamber (with inner dimensions 605×250×250 mm), at an average heating rate of 14 ºC/min; the second stage of the test procedure, in which the coupons' temperature was kept constant at the predefined target temperature, consisted of loading the test specimens up to failure using an *Instron* universal testing machine (load capacity of 250 kN) under displacement control, at an approximate speed of 0.3 mm/min.

The control of the test specimens' temperature, as well as the air in the thermal chamber, was made by means of type K thermocouples (0.25 mm conductor diameter). Regarding the coupons, the thermocouples were installed inside a drilled hole, made along the length of the specimen (17.5 mm of depth; 0.25 mm of diameter).

The displacements at different points of the test specimens during the loading stage were measured using a videoextensometry technique (**Fig. 3 b**). The equipment used consisted of a high definition *Sony* video camera (model *XCG-5005E*, *Fujinon – Fujifilm HF50SA-1* lens), a tripod, where the camera was fixed, and a computer software (*LabView*). This image technique required defining in the test specimens a certain number of contrasting marks (targets), as shown in **Fig. 1**, allowing to track the targets' position at each instant (and for each load level); with the targets' coordinates (x,y), it was possible to compute the specimen's displacement and, subsequently, to determine the corresponding strain. Distortion in each data point was calculated according to **[10]** and shear modulus was estimated by the slope of the stress-distortion curves between 25 and 50% of the maximum shear stress.

During the tests, the load applied by the test machine and its cross-head displacement was also monitored.

The experimental campaign included five series at different temperatures, for which at least three specimens were tested.

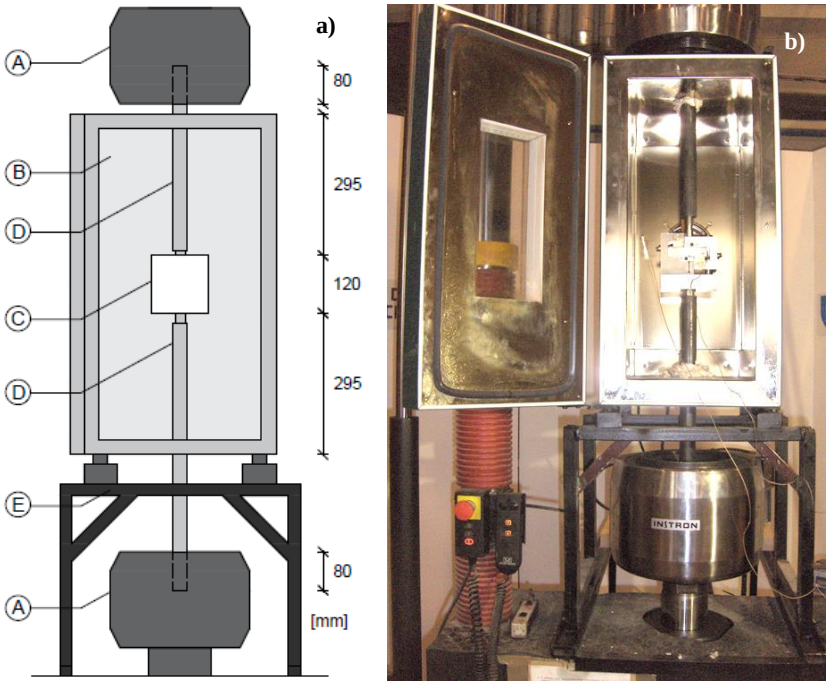

Fig. 2: a) Shear tests setup - A) test machine grip, B) thermal chamber, C) test fixture, D) metal spindle, E) metal structure to support the thermal chamber; **b)** general view of test setup and equipment.

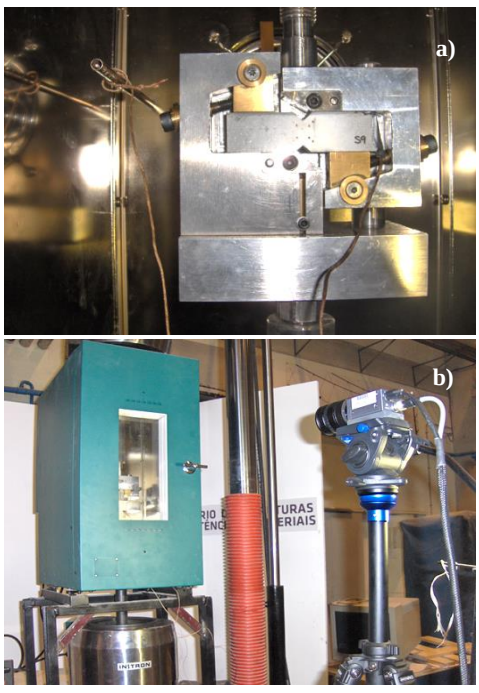

Fig. 3: Details of the test setup: **a)** test fixture and thermocouples; **b)** thermal chamber and video extensometer.

2.3. Compressive tests at elevated temperature

The compressive tests were carried out on 120 mm high I-section short columns.

As for the shear tests, the displacements in different points of the columns' webs were measured using videoextensometry. To that end, the specimens were marked with a set of targets, as shown in **Fig. 4 a**, allowing to track their position during the tests.

The test setup adopted in the compressive tests is illustrated in **Fig. 5**, where it can be seen the thermal chamber used to heat up the specimens (the same equipment used in the shear tests); this thermal chamber was positioned on a *Inepar 3000* testing machine (as depicted in **Fig. 5**) with a loading capacity of 3000 kN. Each test specimen was positioned inside the thermal chamber between two grooved steel plates with 30 mm deep grooves (**Fig. 4 b**), therefore the free height of the short columns was 60 mm (**Figs. 4 a and 5 a**). As shown in **Fig. 5 a** and **Fig. 5 b**, these grooved steel plates were fixed to steel rods (45 mm diameter) by means of cylindrical steel blocks (75 mm height and 100 mm diameter). The upper cylindrical block was positioned under a *Novatech-800-14329* loading cell (loading capacity of 800 kN) and the lower cylindrical block was bolted to the reaction frame of the test machine.

The test procedure was similar to that adopted for the shear tests: the specimens were first heated up to a predefined temperature ranging from ambient temperature to 180 ºC (26 ºC, 60 ºC, 100 ºC, 140 ºC or 180 ºC) at an approximate thermal chamber heating rate of 17 ºC/min; subsequently, and at constant temperature, a compression load was applied up to failure under load control at an average speed of 2.3-2.7 kN/s. The tests were performed using the testing machine mentioned above, controlled with a *Walter + Bai* pressure unit.

The relative vertical displacement between the test machine's plates was measured using two displacement transducers from *TML* (with strokes of 10 and 25 mm, respectively for the top and bottom transducers) positioned as depicted in **Fig. 5 a**.

As in the shear tests, the temperature in the specimens and in the thermal chamber was measured with type K thermocouples. The specimens' thermocouples were installed inside drilled holes made on the columns' web (with 2.5 mm diameter and 4 mm depth - half-thickness) and fixed with a two component polyester resin.

For each temperature series, at least three specimens were tested. During both test stages, temperatures, applied load, displacements of the testing machine's plates and target coordinates (x,y) of the specimens were recorded.

The use of videoextensometry to evaluate the displacements of the specimens during loading presented significant advantages when compared to the displacement transducers, as it allowed to measure the displacements at the free height of the columns, thus avoiding measuring errors introduced by the local crushing of the specimens at the grooved steel plates.

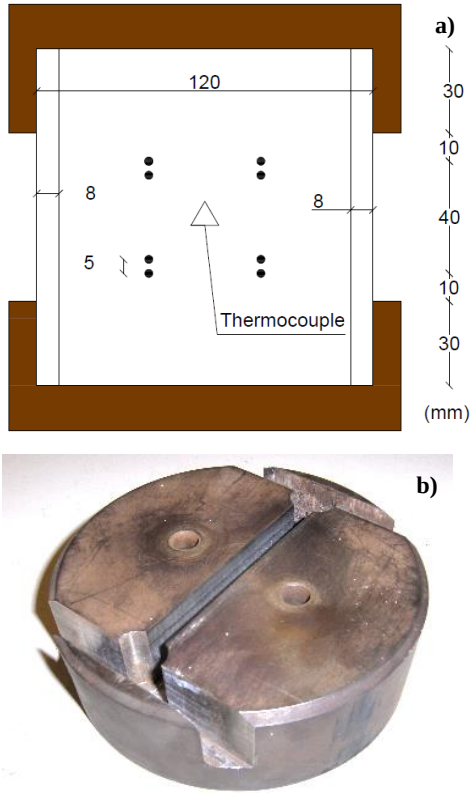

Fig. 4: a) Compression coupons – dimensions and target scheme; **b)** grooved steel plate.

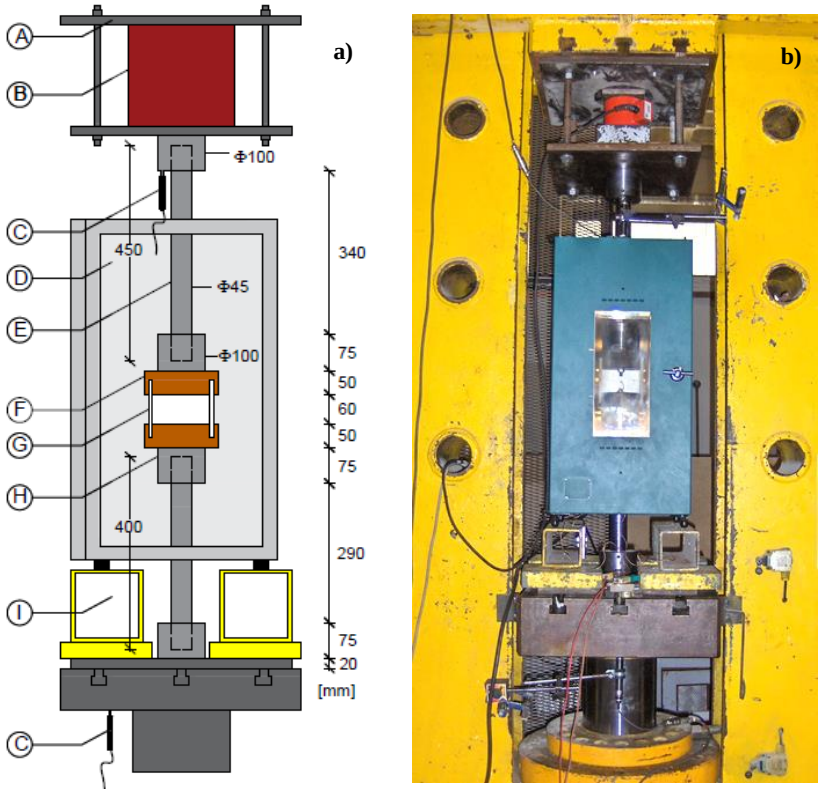

Fig. 5: a) Compressive tests setup – A) metal structure for load cell support, B) load cell, C) displacement transducer, D) thermal chamber, E) steel rod, F) grooved steel plates, G) GFRP specimen, H) cylindrical steel block, I) steel profile for thermal chamber support; **b)** general view of test setup and equipment.

3. Experimental results and discussion

3.1. Shear tests at elevated temperature

Fig. 6 presents the load-displacement curves (total displacement of the testing machine) for one representative specimen of each target temperature, corresponding to an intermediate curve obtained within each series. For all temperatures, the curves presented an approximately linear behaviour at an initial stage of the tests; for higher load levels, the slope of curves (corresponding to the global stiffness of the specimens and the test setup) decreased progressively up to maximum load is attained. This figure also shows that the global stiffness and maximum loads presented a considerable reduction with temperature. It can be observed that for temperatures lower than 100 ºC, the load decreased abruptly after the maximum value is attained. However, for higher temperatures, in particular above T_g, the post-peak behaviour of the curves changed – the load values presented a slight decrease that seems to stabilize.

This behaviour may be explained by the following phenomena: (i) with increasing temperatures the material presents more viscosity and, therefore, a higher deformation capacity; (ii) the measured (total) displacements included the effect of the crushing phenomenon observed in some of tested specimens (discussed below), mostly at 140 ºC and 180 ºC. Regarding the global stiffness, it presented reductions of 50% at 100 ºC and 85% at 180 ºC, when compared to the global stiffness at ambient temperature. This significant stiffness degradation with temperature is mostly due to the matrix softening, which occurs during the glass transition process.

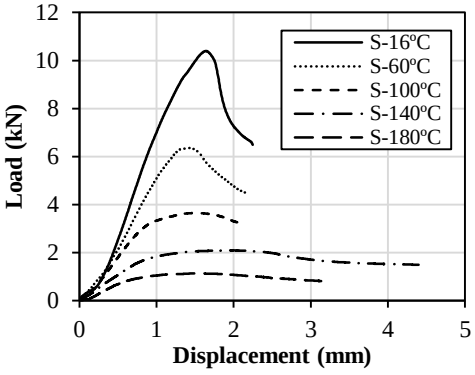

Fig. 6: Load-displacement curves in shear for representative specimens of all tested temperatures.

Fig. 7 shows the shear stress-distortion curves for representative specimens of all tested temperatures. Below 100 ºC, the behaviour is approximately linear until the maximum stress is attained. However, for higher temperatures, the constitutive relationships present a nonlinear behaviour which is due to: (i) the possible debonding of the superficial layers of the GFRP material (especially at 180 ºC), which seems to have affected the video extensometer readings, and (ii) the influence of the testing conditions related to lighting and (low) visibility to the interior of the thermal chamber. Nevertheless, the curves obtained showed a steep reduction of the shear strength with temperature, as depicted in **Fig. 8**, where the shear strength and modulus are plotted as a function of temperature.

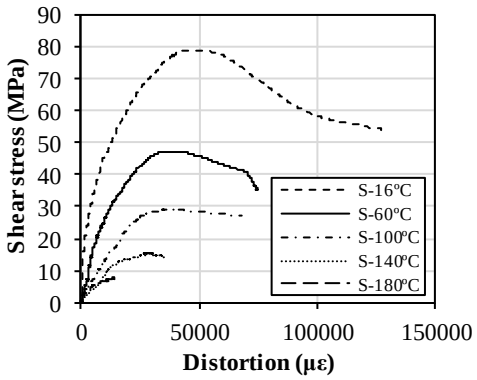

Fig. 7: Shear stress-distortion curves for representative specimens of all tested temperatures.

Regarding the shear strength, the results showed in **Fig. 8** exhibit a reduction of 39% at only 60 ºC (compared to the shear strength at ambient temperature), with that reduction increasing to 88% at 180 ºC. It is worth mentioning that the failure mode observed in specimens tested at 180 ºC was different to those observed at lower temperatures (as discussed below); for this reason, the results obtained at 180 ºC can only be considered as a lower bound of the shear strength at that temperature.

The slope of the linear branch of the shear stress-distortion curves, representative of the shear modulus, presented a progressive reduction with increasing temperatures. As plotted in **Fig. 8**, the shear modulus exhibits a reduction of 77% at 140 ºC, compared to ambient temperature. At 180 ºC, this property increased (significantly) when compared to that at 140 ºC; this unexpected inversion in the degradation trend is possibly due to the fact that at 180 ºC the debonding of the superficial layer of the specimens was more pronounced, therefore affecting more severely the readings of the video extensometer.

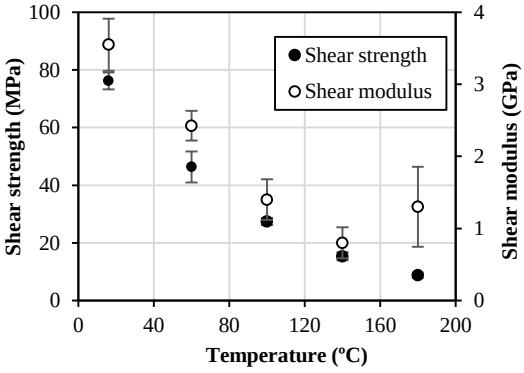

Fig. 8: Shear strength and shear modulus as a function of temperature (average ± standard deviation).

Two different failure modes were observed in specimens tested in shear (**Fig. 9**): (i) for temperatures up to 100 ºC, failure was due to shear in the central section of the specimen, with rupture of the matrix and superficial mats (**Fig. 9 a**); (ii) at 180 ºC, and in some specimens tested at 140 ºC, failure

occurred due to ply delamination and crushing on the central section of the specimens, near the V-notches, as showed in **Fig. 9 b**. The latter failure modes might have occurred due to (i) the low compressive strength of the GFRP material at those temperatures and (ii) the influence of the test setup itself.

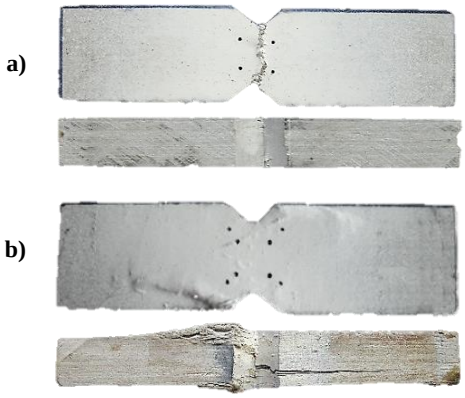

Fig. 9: Typical failure modes of specimens tested, in shear, at: **a)** temperatures below 100 ºC (shear failure); **b)** temperatures above 140 ºC (failure by crushing and ply delamination).

Fig. 10 plots a comparative analysis of the results obtained in the present study in terms of normalized shear strength with the experimental data obtained by Bai & Keller **[4]** and Correia *et al.* **[2]** (previously described in section **1**). This figure shows that the results obtained in the present study exhibited a steeper reduction with temperature and a lower scatter when compared to those from the literature. This difference may be due to the lower susceptibility of the tensile strength to increasing temperature; as mentioned, note that Bai & Keller and Correia *et al* performed 10º off-axis tensile tests, therefore their specimens were subjected to both shear and tension.

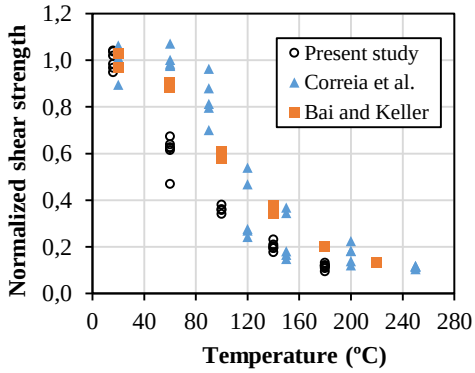

Fig. 10: Comparison of the average normalized shear strength reduction with temperature: present study and results obtained by Bai & Keller [4] and Correia *et al.* [2].

3.2. Compressive tests at elevated temperature

Fig. 11 presents the load-displacement curves (total relative displacement between the plates of the testing machine) for one representative specimen of each target temperature, corresponding to an intermediate curve obtained within each temperature series. For all temperatures, the curves present an initial non-linear branch, which is due to the specimens' adjustment to the grooved steel plates. After this initial stage, and for higher load levels, the material presents an approximate linear behaviour up to failure. The curves plotted in **Fig. 11** show, as expected, progressive global stiffness and maximum load reductions with temperature, which can be explained by the glass transition process underwent by the matrix; the global compressive stiffness at 180 ºC presented a residual value of 38%, compared to that at ambient temperature.

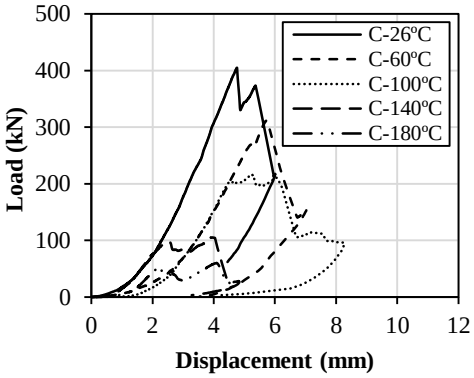

Fig. 11: Load-displacement curves in compression for representative specimens of all tested temperatures.

Fig. 12 presents representative curves of the axial stress-strain relation obtained in specimens tested at ambient temperature (26 ºC), 60 ºC and 100 ºC (these curves were plotted only up to the failure of the specimens). The curves plotted in **Fig. 12** exhibit an initial irregular branch, which can be attributed to the adjustment of the specimens to the grooved steel plates and also to the influence of such adjustment on the accuracy of the video extensometer readings. After this initial stage, the curves exhibited a relatively linear response, presenting a progressive stiffness reduction in the brink of failure; in some cases, especially at 100 ºC, the curves presented an irregular branch prior to failure – such behaviour may be explained by the wrinkling of the material (that characterizes the specimens' failure mode), which also affected the video extensometer readings. Despite the experimental campaign had included tests up to 180 ºC, the stress-strain curves obtained for specimens tested at 140 ºC and 180 ºC presented an erratic behaviour; such unexpected result might have been related to the already mentioned debonding of the material's superficial layer, which was more pronounced at those temperatures.

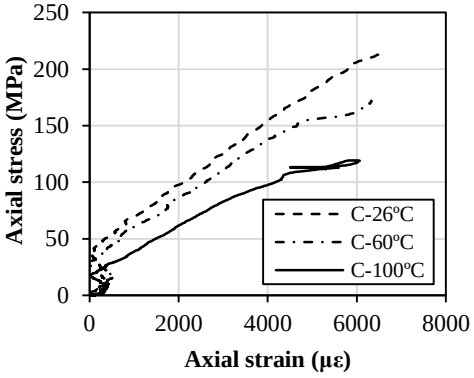

Fig. 12: Axial stress-strain curves for representative specimens tested at 26 ºC, 60 ºC and 100 ºC.

Fig. 13 plots both the longitudinal compressive strength and elasticity modulus in compression as a function of temperature. The compressive strength exhibits reductions of 55% and 87% at 100 ºC and 180 ºC, respectively, therefore confirming the susceptibility of this property to elevated temperature. Regarding the elasticity modulus, it presented reductions of 13% and 19% (compared to ambient temperature) at 60 ºC and 100 ºC, respectively.

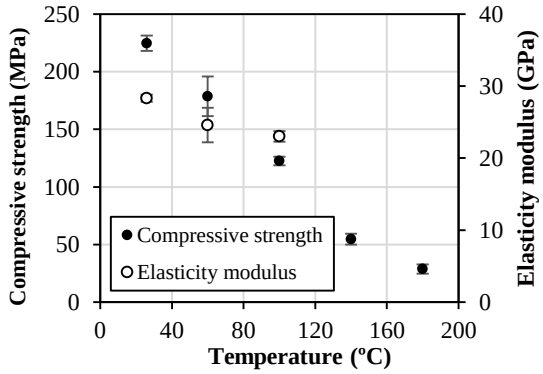

Fig. 13: Compressive strength and elasticity modulus as a function of temperature (average ± standard deviation).

Fig. 14 shows the failures modes obtained in the compressive tests. At ambient temperature (**Fig. 14 a**), failure occurred due to GFRP crushing at the grooved steel plates, with the specimens also presenting signs of delamination of the strand mats. At elevated temperatures, failure occurred firstly by crushing of the cross-section at the grooved plates, which was followed by wrinkling of the material within the free height of the specimens (**Fig. 14 b and c**). This latter phenomenon was triggered by the softening of the resin (that occurs during glass transition), which loses most of its capacity to confine the fibres, leaving them more likely to buckle or kink. This failure mode can be clearly seen in **Fig. 14 c**, which shows a significant detachment of the fibres at 180 ºC.

Fig. 14: Typical failure modes of specimens tested, in compression, at: **a)** 26 ºC, **b)** 60 ºC, 100 ºC and 140 ºC, **c)** 180 ºC.

Fig. 15 plots the normalized compressive strength obtained in the present study together with the experimental data obtained by Bai & Keller **[4]**, Correia *et al.* **[2]** and Wang *et al.* **[5]** (previously described in section **1**). The results obtained in the present study exhibited a less pronounced reduction with temperature than those reported by the above mentioned authors, especially within the 60-100 ºC range; for higher temperatures, all experimental data present similar reductions with temperature.

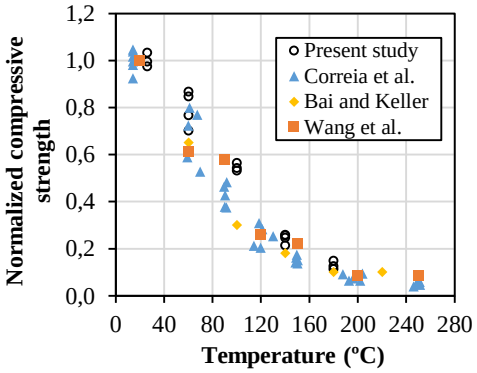

Fig. 15: Comparison of the average residual compressive strength: results obtained in the present study and those from Correia *et al.* [2], Bai & Keller [4] and Wang *et al.* [5].

The failure modes obtained in the above mentioned studies at elevated temperatures were similar to those observed in the present study: rupture occurred at mid-height of the specimens by crushing and wrinkling of the material, which also involved ply delamination. At ambient temperature, the specimens tested by the authors mentioned above exhibited a similar rupture to that described previously, but concentrated in the zones in contact with the grooved plates. However, in the present study, the specimens did not present any wrinkling in those zones; this might have been due to the smaller gap between the grooves and the specimens (thus avoiding such wrinkling). Moreover, the grooves in the steel plates used in the present study were deeper than those used in the tests of Correia *et al.* and Bai & Keller (30 mm *vs.* 5 mm grooves), thus increasing the confinement effect and avoiding the material wrinkling.

4. Modelling of properties degradation with temperature

4.1. Description of models and parameter estimation

A limited number of studies have proposed different models, based on mathematical formulations, to simulate/predict the mechanical properties of FRP materials at elevated temperatures. In **[2]**, Correia *et al.* have shown the accuracy of a set of models, reported here, which were able to successfully describe the tensile, compressive and shear strength degradations with temperature of GFRP pultruded profiles. In the present paper, the experimental results presented in section **3** (namely, in terms of shear and compressive strength, as well as of shear modulus) and in section **1**, were used to assess the accuracy of the models reported in **[2]**, namely the empirical models developed by Gibson *et al.* **[11]**, Mahieux *et al.* **[12]**, Wang *et al.* **[13]** and

Correia *et al.* **[2]**. The above mentioned models encompass curve fitting procedures to the experimental data, unlike the semi-empirical model proposed by Bai and Keller **[14]**, which will also be assessed in the present paper.

In the model of Gibson *et al.* **[11]**, the variation of a generic mechanical property P with temperature T, can be described by the following equation,

$$P(T) = P_u - \frac{P_u - P_r}{2} \times (1 + \tanh[k'(T - T_{g,mech})]) \quad (1)$$

where P_u is the property at ambient temperature and P_r is the property after glass transition (but before decomposition); $k'$and $T_{g,mech}$ are parameters obtained by fitting to the experimental data.

According to Mahieux *et al.* **[12],** a mechanical property can be computed as a function of temperature through the following equation, based on Weibull distribution,

$$P(T) = P_r + (P_u - P_r) \times \exp[-(T/T_0)^m] \quad (2)$$

in which T_0 is the relaxation temperature and m is the Weibull exponent, both of them numerically fitted to the experimental data.

Wang *et al.* **[13]** suggested the following model, which although being initially developed for metallic materials, revealed to be suitable to describe the tensile behaviour of carbon fibre reinforced polymer (CFRP) pultruded laminates at elevated temperature,

$$P(T) = P_u \times \left[A - \frac{(T - B)^n}{C}\right] \quad (3)$$

where the parameters A, B, C and n, to be fitted to the experimental data, can be estimated for different temperature ranges.

As Correia *et al.* mentioned in **[6]**, the rational modelling approach developed by Bai *et al.* **[15]** for the elasticity modulus is extensible for modelling the strength degradation with temperature of GFRP materials since, according to the authors, the strength value during glass transition stems from the contribution of the material's state before and after the glass transition process. This approach was later demonstrated on Bai and Keller's semi-empirical model **[14]**,

$$P(T) = P_g \times [1 - \alpha_g(T)] + P_l \times \alpha_g(T) \times [1 - \alpha_d(T)] + P_d \times \alpha_g(T) \times \alpha_d(T) \quad (4)$$

in which P_g, P_l and P_d, are the materials properties (strength or modulus) in the glassy, leathery and decomposed states, respectively. The parameters α_g and α_d (varying between 0 and 1) correspond to the glass transition and decomposition degrees, respectively, and can be determined from DMA and TGA tests, respectively (in the present study, these parameters were estimated from the tests performed by Pires in **[16]** in a GFRP material similar to that used in the experiments conducted in this study).

More recently, Correia *et al.* **[2]** suggested the following model based on Gompertz statistical distribution,

$$P(T) = (1 - e^{Be^{C \times T}}) \times (P_u - P_r) + P_r \quad (5)$$

where B and C are parameters obtained from fitting the modelling curve to the experimental data.

4.2. Results and discussion

The modelling curves presented in this section were fitted to the experimental results described in section **3**; in addition to those, the results of the shear and compressive strength degradations with temperature available in the literature were also used to further validate the models. The data set, from now on denominated as "full sample", combined the experimental data obtained in the present study for the shear strength, with those from Correia *et al.* **[2]** and Bai and Keller **[4]**. In terms of compressive strength, the full sample included data from the above mentioned authors, together with those from Wang *et al.* **[5]**. The present campaign also allowed studying the shear modulus degradation with temperature; this property was also modelled herein. It is worth mentioning that the shear modulus results reported in **[2]** (reviewed in section **1**) were not obtained from specimens under a pure shear state, as those tests combined shear and tensile stresses; for this reason (and also because the authors reported difficulties in the strain rosette measurements), those results were not included in the present modelling.

For the empirical models, the theoretical curves were obtained by fitting the experimental data using a standard procedure that minimizes the mean square errors to the experimental results. For the model of Bai and Keller, as it is semi-empirical, the definition of modelling curve only required the parameters presented in **Eq. (4)**, which corresponded to experimental results. The accuracy of the curves adjustment to the experimental data was evaluated by the value of the absolute mean percentage error (AMPE).

Fig. 16 to **Fig. 20** plots the variation with temperature of the normalized experimental values of shear strength, shear modulus and compressive strength, together with the modelling curves obtained by the numerical procedure described above.

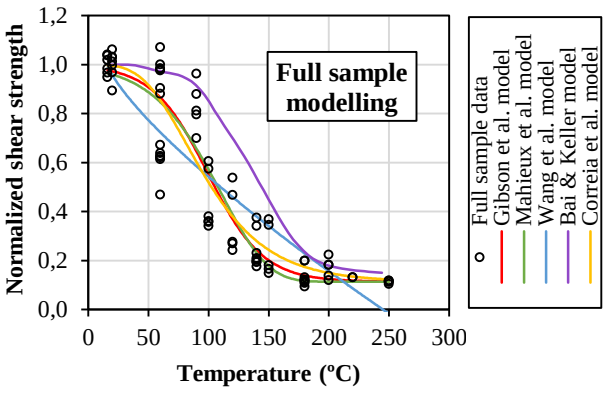

Fig. 16: Normalized shear strength *vs.* temperature: experimental results (full sample) and modelling curves.

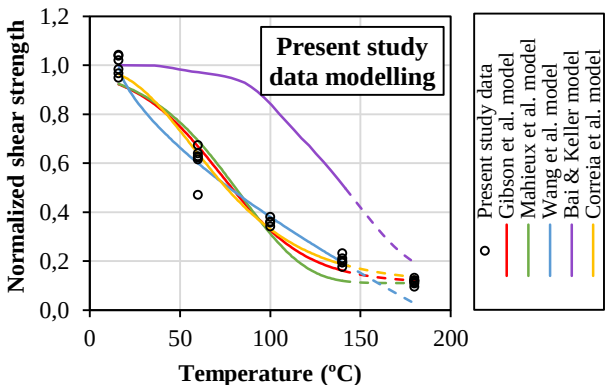

Fig. 17: Normalized shear strength *vs.* temperature: experimental results (present study data) and modelling curves.

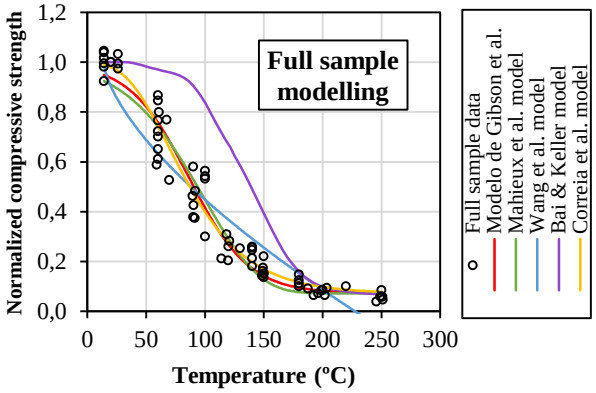

Fig. 18: Normalized compressive strength *vs.* temperature: experimental results (full sample) and modelling curves.

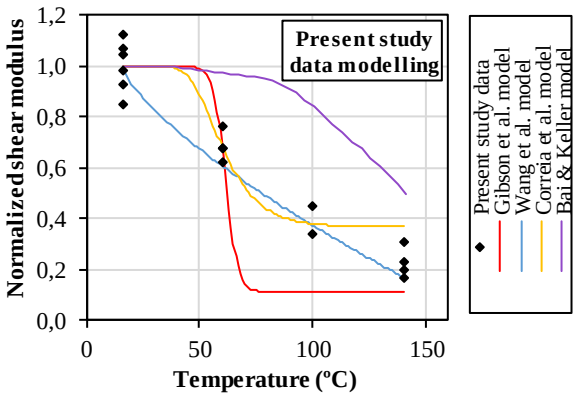

Fig. 19: Normalized shear modulus *vs.* temperature: experimental results (present study data) and modelling curves.

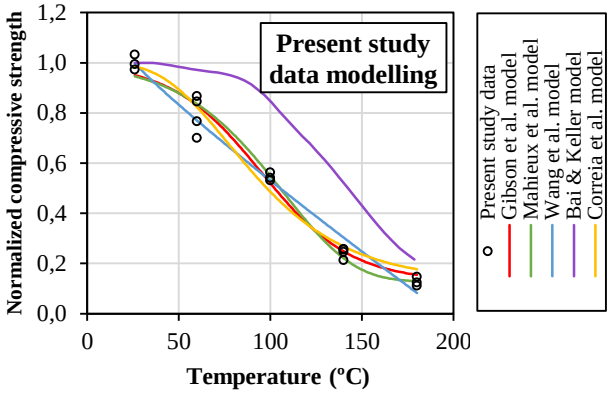

Fig. 20: Normalized compressive strength *vs.* temperature: experimental results (present study data) and modelling curves.

In general, and regardless of the sample considered, the modelling curves presented a good adjustment to the experimental data, indicating that the models were able to provide reasonably accurate estimates of the modelled properties. The semi-empirical model of Bai & Keller **[14]** simulated with less accuracy the material's properties variation with temperature, as confirmed by the higher AMPE value listed in **Table 1**.

Regarding the full sample data, the model of Gibson *et al.* **[11]** provided the most accurate estimates for the shear and compressive strength degradations with temperature, whereas for the compressive and shear strength data obtained in the present study, the models of respectively Mahieux *et al.* **[12]** and Wang *et al.* **[13]** were the most accurate. Further information regarding the modelling curves and the corresponding defining parameters are available in the author's master dissertation.

Table 1: Simulation of GFRP mechanical properties – parameter estimation and absolute mean percentage error (AMPE) for different models.

Model	**Parameter**	**Shear strength**		**Shear modulus**	**Compressive strength**	
	Sample	Present study	Full sample	Present study	Present study	Full sample
Gibson *et al.* [11] Eq. (1)	k' (-)	0.0207	0.0218	0.1907	0.0203	0.0197
	$T_{g,mech}$ (ºC)	72.52	99.32	61.55	94.98	86.50
	AMPE (%)	12.3	21.3	27.3	9.0	17.7
Mahieux *et al.* [12] Eq. (2)	m (-)	11	11	-	11	9
	T_0 (K)	360.04	387.47	-	384.02	377.43
	AMPE (%)	19.6	21.7	-	7.7	19.9
Wang *et al.* [13] Eq. (3)	A (-)	1.00	1.00	1.00	1.00	1.00
	B (-)	16.00	16.00	16.00	26.00	14.00
	C (-)	32.06	68.67	38.82	108.99	33.34
	n (-)	0.6745	0.7784	0.7207	0.9142	0.6538
	AMPE (%)	6.2	38.1	13.7	14.7	44.2
Bai & Keller [14] Eq. (4)	AMPE (%)	82.5	48.0	65.3	53.7	67.0
Correia *et al.* [2] Eq. (5)	B (-)	-5.07	-9.13	-149.38	-8.36	-6.63
	C (-)	-0.03	-0.03	-0.09	-0.03	-0.03
	AMPE (%)	7.2	22.8	25.6	13.9	18.1

5. Conclusions

The present experimental and analytical study aimed at (i) characterizing the variation of shear and compressive properties of GFRP pultruded profiles from ambient temperature up to 180 ºC, and (ii) assessing the accuracy and reliability of a set of models, suggested in the literature, to predict the degradation with temperature of those properties. From the results obtained, the following main conclusions can be drawn:

1. As expected, the GFRP mechanical properties presented considerable reductions with temperature, with the shear properties being more susceptible to the thermal degradation than the ones in compression.
2. The shear and compressive strengths were severely reduced for elevated temperatures, presenting strength retentions at 180 ºC of only 12% and 13%, respectively, compared to ambient temperature.
3. The shear modulus exhibited a retention of 23%, compared to ambient temperature, at 140 ºC.
4. In the shear tests performed up to 100 ºC, as expected, the specimens presented shear failure in the central section, with matrix and superficial mats rupture. However, at 180 ºC (and in some specimens tested at 140 ºC), failure occurred due to ply delamination and crushing of the material in the loading/support areas.
5. Despite the efforts to study the variation of the elasticity modulus in compression up to 180 ºC, reliable/valid results were obtained only up to 100 ºC. At that temperature, a retention of 81% was obtained compared to ambient temperature.
6. In the compressive tests performed at ambient temperature, a failure mode characterized by material crushing at the loading plates and delamination of reinforcing layers was observed. At elevated temperatures, failure occurred firstly by material crushing at the plates, followed by wrinkling or kinking of the longitudinal fibres of the web. A significant level of fibre detachment was observed mainly in specimens tested at 180 ºC.
7. The results obtained in both shear and compressive tests, regarding strength and failure modes, are in good agreement with those reported in the literature.
8. The empirical models considered in the present study were able to accurately simulate the variation with temperature of the shear strength, shear modulus and compressive strength; the estimates obtained from the semi-empirical model of Bai & Keller were considerably less accurate.

6. References

[1] Correia, J. R., *Polymeric Matrix Composites* (in Portuguese), in Science and Engineering of Construction Materials (Editors, Margarido, F. and Gonçalves, M. C.), chapter 11, IST Press, Lisboa, 2012.

[2] Correia, J. R., Gomes, M. M., Pires, J. M., and Branco, F. A., *Mechanical behaviour of pultruded glass fibre reinforced polymer composites at elevated temperature: Experiments and model assessment*, Composite Structures, Vol. 98, N. 1, pp. 303–313, 2013.

[3] Mouritz, A. P., Gibson, A. G., *Fire Properties of Polymer Composite Materials*, Springer, Dordrecht, 2006.

[4] Bai, Y., Keller, T., *A kinetic model for predicting stiffness and strength of FRP composites in fire*, Proceedings of the Fifth International Conference of Composites in Fire, Newcastle, 2008 (cited by [2]).

[5] Wang, Y. C., Wong, P. M. H., *An experimental study of pultruded glass fibre reinforced plastics channel columns at elevated temperatures*, Composite Structures, Vol. 81, N. 1, pp. 84–95, 2007.

[6] Correia, J. R., Bai, Y., and Keller, T., *A review of the fire behaviour of pultruded GFRP structural profiles for civil engineering applications*, Composite Structures, Vol. 127, pp. 267–287, 2015.

[7] Morgado, T., Nunes, F., Correia , J. R., and Branco, F., *Fire protection systems for glass fibre reinforced polymer (GFRP) pultruded profiles, Task 5: Full-scale fire resistance experiments on GFRP pultruded structural elements - Dynamic Mechanical Analysis (DMA)*, FCT Project PTDC/ECM/100779/2008, Instituto Superior Técnico, 2012.

[8] Gomes, M. M., Correia, J. R., Pires, J. M., and Branco, F. A., *Fire protection systems for glass fibre reinforced polymer (GFRP) pultruded profiles, Task 3 phase 2: Small-scale tensile tests on GFRP pultruded laminates at elevated temperature*, FCT Project PTDC/ECM/100779/2008, Instituto Superior Técnico, 2012.

[9] Gomes, M. M., Correia, J. R., Pires, J. M., and Branco, F. A., *Fire protection systems for glass fibre reinforced polymer (GFRP) pultruded profiles, Task 3 phase 4: Small-scale compressive tests on GFRP pultruded laminates at elevated temperature*, FCT Project PTDC/ECM/100779/2008, Instituto Superior Técnico, 2012.

[10] ASTM D 5379/D 5379M - 05, *Standard Test Method for Shear Properties of Composite Materials by the V-Notched Beam Method*, West Conshohocken, ASTM, 2010.

[11] Gibson, A. G., Wu, Y., Evans, J. T., and Mouritz, A. P., *Laminate theory analysis of composites under load in fire*, Journal of Composite Materials, Vol. 40, N. 7, pp. 39–58, 2006 (cited by [2]).

[12] Mahieux, C. A. et al., *Property modeling across transition temperatures in PMC 's : Part I - tensile properties*, Applied Composite Materials, Vol. 42, pp. 217–234, 2001.

[13] Wang, K., Young, B., and Smith, S. T., *Mechanical properties of pultruded carbon fibre-reinforced polymer (CFRP) plates at elevated temperatures*, Engineering Structures, Vol. 33, N. 7, pp. 2154–2161, 2011.

[14] Bai, Y., Keller, T., *Modeling of strength degradation for fiber-reinforced polymer composites in fire*, Journal of Composite Materials, Vol. 43, N. 21, pp. 2371–2385, 2009 (cited by [2]).

[15] Bai, Y., Keller, T., and Vallée, T., *Modeling of stiffness of FRP composites under elevated and high temperatures*, Composites Science and Technology, Vol. 68, N. 15–16, pp. 3099–3106, 2008.

[16] Pires, J., *Mechanical Behaviour at Elevated Temperature of Pultruded GFRP Composite Profiles* (in Portuguese), Master dissertation in Civil Engineering, Instituto Superior Técnico, 2012.